

# Effects of Loading Fields on Marine Objects

Kalman Ziha

*University of Zagreb, Faculty of Mechanical Engineering and Naval Architecture, Department of Naval Architecture and Ocean Engineering, Zagreb, Croatia*

---

This technical note evokes directionally nonuniform loading field effects on exposures of marine objects and structures in service under environmental conditions. The note firstly reveals the statistical variability of distributions of probabilities and the entropy concept of uncertainty of systems of events for identification, ordering and presentation of probabilistic seasonal nonuniformities of wind wave loading fields. This paper provides diagram of variability of wind wave directions and the chart of ocean-wide directional nonuniformities compiled from the Global Wave Statistics (GWS). It also considers seasonal loading field distributions of wind wave heights against wave directions as well as methods for calculation and presentation of directional exposabilities of marine objects and structures. The study introduces two methods for favorable placement and selection of sustainable directions of marine objects and structures exposed seasonally to nonuniform wind wave loading fields based on criteria for minimal average exposure and on robust uniform exposures during service period. The note elaborates examples of favorable placement of a marine object on six piles near the east Brazilian coast and of an oil tanker in the Gulf of Mexico. The note at the end illustrates the use of the multiple-criteria approach either to support decisions about optimal placement and sustainable headings to waves or for avoidance of unfavorable directional field effects and their combination on marine objects and structures.

**Keywords:** ship motions; ocean engineering; operations; safety; weather; waves; loads

---

## 1. Introduction

DIRECTIONALLY NONUNIFORM loads seasonally or instantaneously influence the superstructures and the underwater bodies of stationary and moving marine objects and structures under environmental effects of waves, winds, currents, ice, or tidal and temperature fluctuations. The nonuniform loading fields affect functional or operational efficiency, structural integrity, general safety, and vulnerability as well as limit strength and fatigue endurance. The selections of a location or of a position after translocation of marine objects and the selection of the courses for moving structures with respect to directionally variable loading fields are important decisions in marine technology and shipping that involve several criteria, and each of them can affect the overall lifetime fitness for service.

The study at the beginning considers the statistical uncertainty measures for wind wave directions and reminds at the probabilistic entropy due to its potential in assessment of uncertainties of wind wave loading directions (Ziha 2000a, 2000b, 2007). The entropy concept emerged earlier in the information theory for the evaluation of the amount of information (Wiener 1948, Shannon & Weaver 1949). This was later generalized in the probability theory and statistics (Khinchin 1957, Renyi 1970, Aczel & Daroczy 1975) as the probabilistic uncertainty measure for systems of random events.

Many researchers contributed to sophisticated analytical methods for marine objects and structures such as wave-induced loads (Noblesse & Yang 1993, Guedes-Soares 2003), deep water mooring (Mavrakos et al. 1996, Sii et al. 2005), wave kinematics in regular and irregular seas (Gudmestad 1993), wave, wind, and current data for the design of marine structures (Ewing 1990), lateral loads (Belenkiy et al. 2001), limit states (Paik 2006) that sometimes involve additional uncertainties. Many recent books are devoted to history, function, loading, design, construction,

---

Manuscript received by JSPD Committee October 2009; accepted April 2010.

dynamics, reliability, damage, and maintenance of marine structures such as Wilson (2002), Paik and Thayamballi (2007), and Gerwick and Morris (2007).

The study in the continuation considers the directional exposable of marine objects to external influences as an important property that can relate the exposure of structures to directional field effects. Applications of directional exposures to wind wave loading field effects and their combinations on the local and global level are elaborated on in examples of the lateral dynamic loads, motions, and strength of marine structures. Different decision-making techniques (e.g., Bernard 1996, Collette & Siarry 2004, Yoon & Ching-Lai 2006) are to be applied for combined influence of more than one important field effect on structural behavior in order to decide on favorable and compromising directions or on avoidance of nonfavorable service conditions.

The motivating aim of this study is to investigate in addition to the important general engineering and common construction issues regarding safety and efficiency, how the application of the structural exposable can provide practical recommendations for seasonally adequate placement of marine equipment and safer service of ships that complies with marine experience about exposures to directionally nonuniform loading fields and can help in designing and operations of marine structures.

## 2. Tracing the ocean wind wave loading field's directional nonuniformities

Visual observations of commercial ships have been archived for a century and a half starting in 1861, and since 1961 the collection is systematic according to a resolution of the World Meteorological Organization (WMO) using the past experiences to eliminate biases. The compilation of visual observations of commercial ships in the Global Wave Statistics (GWS) prepared by Hogben et al. (1986) is one of the important sources for investigation of wind wave loading field effects on marine structures on the global level. The observations in GWS are presented in  $N_A = 104$  Marsden's square areas  $A$  (see Appendix), for overall and  $N_d = 8$  principal directional classes denoted  $d_j = (\text{all}), NW, N, NE, W, E, SW, S, SE, j = 1, 2, \dots, 8$  sectors of 45 degrees from which the waves concerned were coming. The GWS data are available for annual and  $N_s = 4$  seasonal observations denoted  $s = (\text{annual}), \text{March-May (MM)}, \text{June-August (JA)}, \text{September-November (SN)}, \text{December-February (DF)}$ .

The GWS integrated the wind/wave climate observations on global level in scatter diagrams of joint distributions of  $N_h = 15$  significant wave heights in meters and  $N_t = 11$  wave periods in

seconds. The advantages of the GWS are the global approach and the duration of the collection period. The GWS do not account directly for highly localized climate conditions such as the size of the region, the topography within/surrounding of the region, the fetch, and ocean surface currents particularly outside the considered oceanic areas. Consistency of climatological data of particular importance for local conditions was attained by careful seasonal subdivisions throughout any given area. Monthly frequency tables of wave heights and wind forces against directions, together with information on rough weather including ice conditions and occurrence of tropical cyclones were used to decide on seasonal subdivisions in the GWS. Thus, extreme conditions and rough weather data are indirectly included in seasonal observations in GWS. It was not possible to ensure uniform distribution of ship's observations in GWS over all sea areas over the world over the years 1854 to 1984. The density of observations is much greater along major shipping routes. In some areas, the numbers of seasonal and directional joint wave and wind observations provide insufficient data for statistical analysis. The area subdivision covers most of the continental shelf where offshore and coastal engineering activities are concentrated and the majority of important routes of shipping or long-haul towing. Probabilities of extreme conditions or rough weather that are possibly not covered by the GWS have to be accounted for when considering marine operations in the field.

The commonly applicable views on the loading field's non-uniformities use statistical distribution of wave data as random variables. In addition, the study employs descriptive statistical variability measures for dispersions of observed probabilities of wind wave directional  $d_j, j = 1, 2, \dots, 8$ . If not all the wave direction probabilities are known, which is often the case in GWS, then the probability

$$p_{A_i} \leq \sum_{j=1}^8 d_j$$

of available observed wave directions in an area  $A_i$  is not necessarily equal to unity.

The statistical variability can be viewed as the range  $d_{\min} - d_{\max}$  or more appropriately as the variance

$$V(A_i) = \sigma^2(A_i) = \sum_{j=1}^8 [d_j - d_{\text{mean}}]^2$$

where  $d_{\text{mean}} = p_{A_i}/8$  is the mean value of seasonal probabilities of wind wave directions in an area.

The coefficient of variation is the relation of the standard deviation and the mean value that represents the variability in numbers of wave directions in an area  $A_i$ :

## Nomenclature

$CV$  = Coefficient of variance of wave directions in an area  
 $c$  = exposable factor  
 $D$  = probability of encountering wave directions in the field (GWS); average number of wave directions in the field  
 $E$  = directional exposure to field effects ( $F \times S$ )  
 $e$  = distribution of directional exposures ( $E/\Sigma E$ )  
 $F$  = field directional intensity  
 $H$  = entropy of wave directions in the field ( $\Sigma d \log d$ )  
 $H_e$  = effective field wave height  
 $R$  = redundancy (uncertainty) ( $\Sigma e \log e$ )

$p$  = interaction factor  
 $S$  = overall exposable of a structural property ( $\Sigma s$ )  
 $s$  = elementary exposable of a structural property  
 $V$  = variance of wave directions in an area  
 $w$  = influencing factor  
 $\Phi$  = field direction  
 $\Lambda$  = elementary structural property direction  
 $\Omega$  = structure direction  
 $\Theta$  = structure direction to the field ( $\Omega - \Phi$ )

$$CV(A_i) = \sqrt{V(A_i)}/d_{\text{mean}} = 8 \cdot \sqrt{V(A_i)}/p_{A_i} \quad (1a)$$

The study presents the variability in equation (1a) of all GWS areas (Fig. 1). The low coefficient of variation of wave wind directions indicates more uniform loading fields. Thus,  $CV(A_i) = 0$  in (1) applies only to fully uniform distribution, that is when  $d = 1/8$  for all directions. High  $CV$  values indicate that there are some dominant directions characterized by high  $d_j \gg$  for some particular  $j$  (Fig. 1).

Equivalent numbers of wave directions with respect to the overall number  $N_d = 8$  indicate the uncertainty due to variability of numbers of wave directions (Fig. 1) and can be defined by using equation (1a) as:

$$D_{A_i}(d) = 8/p_{A_i} - CV(A_i) = 8 \cdot \left(1 - \sqrt{V(A_i)}\right)/p_{A_i} \quad (1b)$$

The study next investigates how the probabilistic uncertainty measures based on the entropy of joint and marginal probability distributions of observed wave heights/periods in principal directions of GWS can orderly and comprehensively trace the loading field's nonuniformities of the ocean wind waves on an annual and seasonal basis (Ziha 2007). The value of  $-\log_2 d_j$  expresses how unexpected a wave direction  $j$  is (Wiener 1948). For incomplete data sets such as is often the case with wave direction observations in GWS, Renyi (1970) proposed the unconditional entropy denoted as the Renyi's entropy of order one whose limiting case is appropriate to incomplete probability distributions. This entropy is applied to the wind wave direction probabilities  $d_j$ ,  $j = 1, 2, \dots, 8$  in an area  $A_i$ , where  $i = 1, 2, \dots, N_{A_i}$ , in the following form:

$$H(A_i) = -\frac{1}{p_{A_i}} \sum_{j=1}^8 d_j \cdot \log_2 d_j \quad (2a)$$

Note how the incompleteness of wave directional observations  $p_{A_i}$  increases the amount of information defined by the Shannon's entropy originally given as the weighted sum of unexpectedness of wave directions:

$$H(A_i) = -\sum_{j=1}^8 d_j \cdot \log_2 d_j$$

for complete systems in equation (2a) where the weights are the probabilities of direction occurrences.

The logarithm in equation (2a) is normally of base two and the unit for entropy is then denoted as one bit.

The maximal entropy in an area  $A_i$  is  $H_{\text{max}}(A_i) = \log_2 8 = 3$  bits for the uniform distribution of wave directions; that is, if all the directional probabilities are equal and amount to  $d_j = 1/8$  for all  $j$  (2). If only one wave direction is observed, its probability equals

unity and all the other probabilities are zero, then the minimal entropy  $H_{\text{min}}(A_i) = 0$  indicates the most nonuniform probability distribution (Fig. 1).

Aczel and Daroczy (1975) mentioned the average number of equally probable events derivable from equation (2a), as:

$$D(A_i) = 2^{H(A_i)}, \quad i = 1, 2, \dots, 104 \quad (2b)$$

The study further employs the concepts in equations (1) and (2) for comprehensive assessment and presentation of the non-uniformity of the distribution of wave directions  $D(A_i)$  in each of the Marsden's squares  $A_i$  by average number of directions in the field. The maximal average number of wave directions  $D_{\text{max}} = 8$  in an area represents the fully uniform distribution with equal probabilities  $d_j = 1/8$  for all  $j$  (3). Other values of  $D \neq 8$  indicate directly the relative ordering of directional uniformities relatively to the original distributions.

There is a principle difference between statistical and probabilistic uncertainty measures considered in the note. The statistical uncertainty measures account for data dispersion of the probabilities of encountering wave directions since the probabilistic measures account for uncertainties related to occurrences of random wave directions. For example, the entropy in equation (2a) of 3 bits expresses the uncertainty of uniform distribution of 8 principal wind wave directions (2b) that is equivalent to the uncertainty of tossing three coins involving 8 possible outcomes, or, the entropy in amount of 1.58 bits expresses the uncertainty of 3 equally probable directions. In both cases, the coefficient of variation in equation (1a) is zero because of the uniform distributions of probabilities of encountering wave directions.

The study next brings forward the wind wave directional non-uniformities in all 104 GWS ocean areas  $A_i$  (Appendix). The paper firstly provides the diagram of wind wave directional uncertainties in all areas  $A_i$ ,  $i = 1, 2, \dots, 104$ , presented by coefficient of variation  $CV(A_i)$  [equation (1a)] and by appropriate equivalent numbers of directions  $D_{A_i}(d)$  [equation (1b)], by entropy  $H(A_i)$  [equation (2a)], and by average number of directions  $D(A_i)$  [equation (2b)] (Fig. 1).

The statistical and probabilistic measures indicate same relative ordering, although they define and present uncertainties of wave directions differently: high  $CV(A)$  [equation (1a)] and low  $H(A)$  [equation (2a)] indicate higher loading field nonuniformities and vice versa (Fig. 1). Equivalent numbers of events  $D_{A_i}(d)$  [equation (1b)] and average numbers of directions  $D(A_i)$  [equation (2b)] are in good agreement (Fig. 1).

The study discusses next the probabilistic entropy concept of average number of equally probable wave directions given by

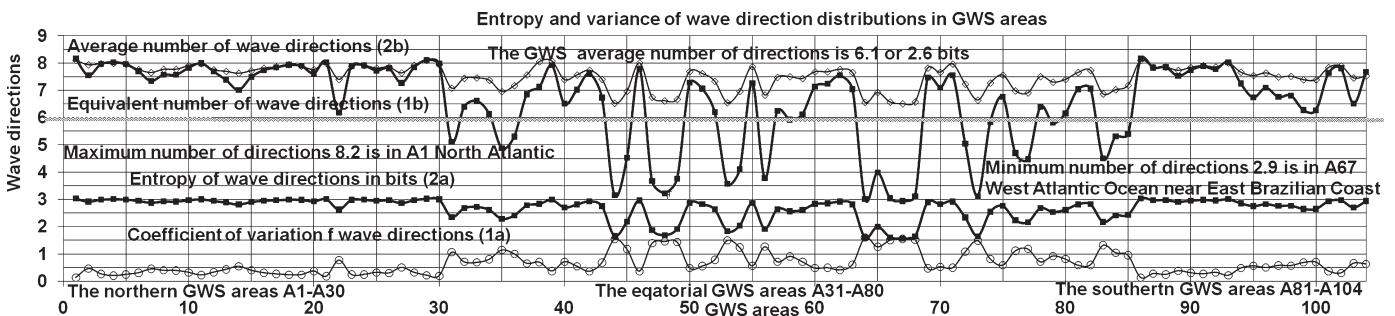


Fig. 1 Oceanwide annual wave directional variabilities [equations (1a) and (1b)] and uncertainties [equations (2a) and (2b)]

8 categories  $D(A_i)$  (2b) from 1 to 8 directions (Fig. 2) as a practical and comprehensive method for presentation of global wind wave loading field nonuniformities in all ocean areas. The entire GWS has an average number of  $D(\text{GWS}) = 6.10$  directions. The minimal wave directional uniformity  $D_{\min} = 2.94$  directions (Fig. 2) is encountered close to the western Brazilian coast [A67] (see Appendix for number in brackets). In this area the east, southeast and south wave directions prevail with more than 90% (Figs. 3a and 3b). The maximal average number of wave directions  $D_{\max} = 8.16$  in Norwegian Sea [A1] even exceed the nominal amount of 8 directions (Fig. 2). In this area, the observed wave directions are almost uniformly distributed but suffer reported data incompleteness for  $p_{Ai} < 1$  in (1, 2) that increases the uncertainty. The chart indicates how the more uniformly distributed wave directional categories of 6 to 8 characterize the northern [A1–A30] and southern [A81–A104] ocean areas. The lower directional categories from 3 to 5 average wave directions are characteristic only to some of the equatorial areas [A31–A80] amidst of Atlantic [A66–A68], Pacific [A44, A64, A73], and Indian [A76, A77] Oceans where the waves are observed in smaller number of directions of 8 (Fig. 2).

The paper next illustrates the seasonal wave wind directional uncertainties and nonuniformities in Caribbean Sea (Table 1) that are covered by GWS area A47 (Appendix), where the average number of observed directions are minimally 3 in period June–August (JA), maximally 4 in period September–November (SN) and 3.7 on annual basis.

### 3. Wind wave directional loading fields

The seasonal distribution  $s$  of directional wind wave loading field  $F_s$  in directions  $\Phi$  and intensity appropriate to wave heights  $H$  is denoted as  $F_s(\Phi, H)$ . The wave direction  $\Phi$  is defined clockwise in the global coordinate axes with respect to principal directions N, NE, E, SE, S, SW, W, and NW or in degrees  $\Phi = 0$  to 360 deg (N-true north). The GWS data represent the best estimate of the probability that the wind-generated components of the seaway will approach from the specified direction ( $\pm 22.5$  deg).

The field intensity is characterized by the waves exceeding a value of wave height  $H_c$ . For example, the distributions of wave directions in Marsden's square A67 for different significant loading field heights on annual bases are given by appropriate loading field intensity distributions  $F_s(\Phi, H_c)$  separately in polar diagram (Fig. 3a) and in normal diagram (Fig. 3b). Note that the area A67 on annual bases has the least number  $D(\text{A67}) = 2.91$  (2b) of average wave directions out of all 8 or 1.54 bits (2a) in the entire GWS (Fig. 1 and Appendix). At the same time the statistical mean value for all wave heights is  $\Phi_{\text{mean}} = 120$  deg with standard deviation of 7 deg.

### 4. Directional exposability of marine objects and structures

The directional exposability of stationary as well as of nonstationary marine objects is considered their external or internal property for being affected during seasonal service (Fig. 4) by local or global effects in any direction of nonuniform loading fields (e.g., Figs. 3a and 3b).

The position of an object or of a structure in global coordinate system can be determined by angle  $\Omega$  starting from the direction North (N-true north) (Fig. 4). The deviations of the angle are denoted  $\pm \Delta\Omega$ . The difference  $\Theta = \Omega - \Phi$  is the angle of the object relative to the direction  $\Phi$  of the field.

The note first investigates the overall directional lateral  $L$  exposability of marine objects or structures denoted as  $S_L(\Theta)$  in direction  $\Theta$  relative to the seasonally variant loading fields  $\Phi$  defined as:

$$\Theta = \Omega - \Phi \quad (3)$$

The lateral exposability is considered the property of exposure to any field direction of all external surfaces of an object to local structural effects such as wave impact loads and lateral pressures. That implies pressure-induced responses in proportion to object's elementary areas  $s_j$  exposed orthogonally to the field in direction  $\Theta$ , such as, for example, local stresses and deflections in shell plating and supporting structures.

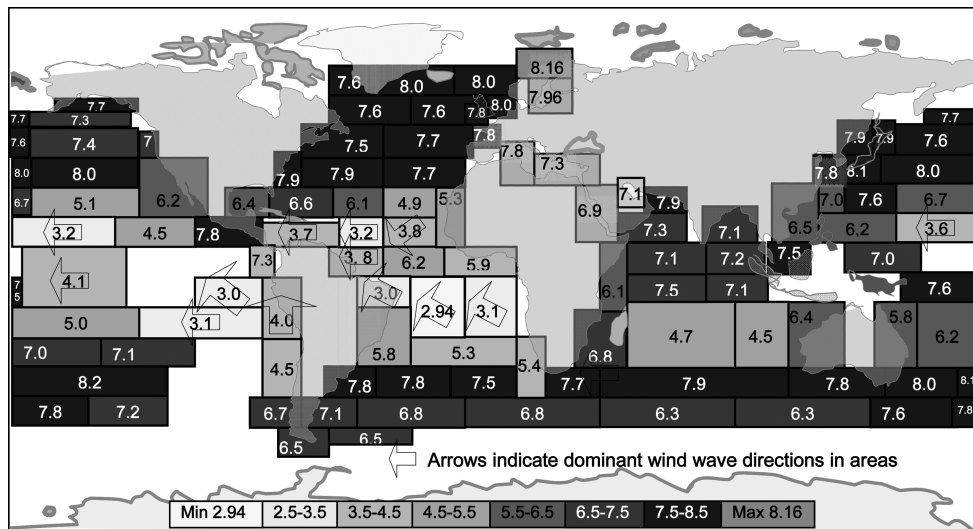
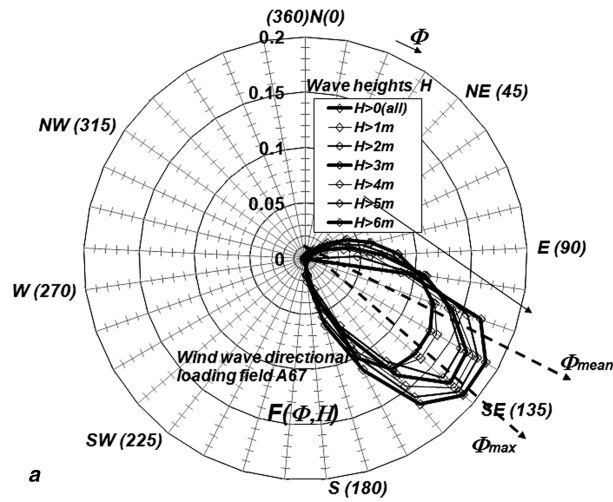


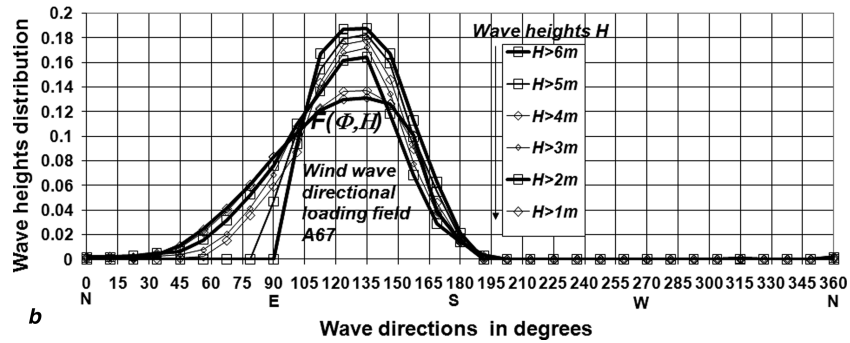
Fig. 2 Chart of average number of wave directions [equation (2b)] observed in GWS on annual basis

Directional distribution of wave heights in GWS area A67



a

Directional distribution of waves heights in GWS area A67



b

Fig. 3 a Polar distribution of wave directions for significant wave heights exceeding a value of  $H_e$  near the east Brazilian coast (Marsden's square A67) on annual bases from GWS. b Distribution of wave directions for significant wave heights exceeding a value of  $H_e$  near the east Brazilian coast (Marsden's square A67) on annual bases from GWS

Table 1 Seasonal distribution of wind wave directions in Caribbean Sea (GWS area A47, Appendix)

d % GWS	Annual	MM	JA	SN	DF
N	3.79	3.63	1.82	4.32	5.28
NE	27.73	28.82	20.93	24.29	36.43
E	51.6	51.27	61.44	47.22	48.39
SE	9.72	10.76	10.4	12.33	5.55
S	2.15	1.78	1.75	3.99	1.14
SW	0.99	0.63	0.85	2.06	0.43
W	1.01	0.81	0.78	1.76	0.72
NW	1.27	1.08	0.78	2.02	1.21
Sum	98.26	98.78	98.75	97.99	99.15
Unknown	1.74	1.22	1.25	2.01	0.85
Total	100	100	100	100	100
CV(A47) (1a)	3.94	3.95	4.52	3.48	4.04
D(d) (1b)	4.20	4.15	3.58	4.68	4.03
H(A47) (2a)	1.88	1.78	1.58	2.02	1.71
D(A47) (2b)	3.67	3.44	2.99	4.05	3.27

Wave direction East (E) is highly dominant in Caribbean Sea.

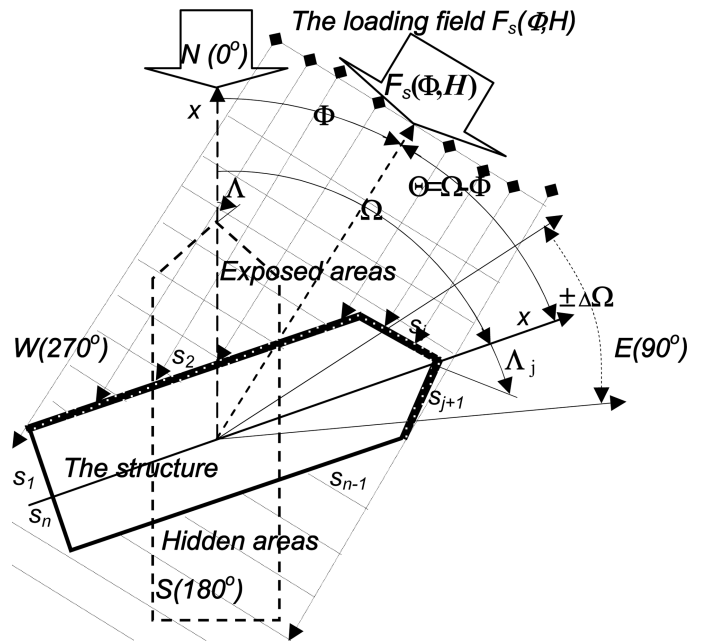


Fig. 4 Directional expositability of objects in loading fields

Elementary areas  $s_j$  are orientated in direction  $\Lambda_j$  with respect to the object's local coordinate axis  $x$  (Fig. 4) and represent parts of the object's laterally exposed surface where the character of exposure might be changing. For an object's angle  $\Omega$ , all the exposed areas  $s_j$  incline relatively to the starting position in amount of  $\Omega + \Lambda_j$ . Therefore, the elementary directional lateral exposability of an area  $s_j$  in direction  $\Lambda$  represents its projection in the field direction  $\Phi$  (Fig. 4) depending on the relative angle between the object and the field  $\Theta$  [equation (3)]:

$$s_j = s_j \cdot \sin(\Omega + \Lambda_j - \Phi) = s_j \cdot \sin(\Theta + \Lambda_j) \quad (4)$$

The overall lateral exposability  $S_L(\Theta)$  in direction  $\Theta$  of an object rotated for an angle  $\Omega$  is the sum of all the exposures of the elementary properties such as loads or responses in proportion  $c_j$  to exposed areas  $s_j$  in the field direction  $\Phi$  [equation (4)]:

$$S_L(\Theta) = \sum_{\text{For all exposed areas}} c_j \cdot s_j \quad (5)$$

The lateral exposability factor  $c_j$  defines the proportion of the elementary property to the exposed area  $s_j$  (5) accounting for the relative effectiveness of any area  $s_j$  with respect to the overall exposability of a structure. When  $c = 1$  for all areas, the overall lateral exposability  $S_L(\Theta)$  [equation (5)] represents the surface exposure of the structure, that is, the projection of the structural surface in the field direction  $\Phi$  (Fig. 4).

The lateral exposability of an optionally rotated fully exposed complex structure comprised of  $k$  distant objects is simply the sum of all individual object exposures  $S_k(\Theta)$  [equation (5)], (e.g., Fig. 6):

$$S_L(\Theta) = \sum_{\text{For all } k \text{ objects}} p_k \cdot S_k(\Theta) \quad (6)$$

The interaction factors  $p_k$  in equation (6) account for the relative importance of each part to the whole structure and for possible interactions among the components.

If the frontally exposed elementary areas (e.g., Fig. 4) and parts of an object (e.g., Fig. 6) accept most of the field impacts, all the hidden elementary areas  $s_j$  [equation (4)] or parts  $S_k$  should be excluded from summation or included with appropriate effectiveness factor  $c_j$  [equation (5)] or weighting factor  $p_k$  [equation (6)].

The sensitivity of exposability of an elementary area  $s_j$  in direction  $\Omega + \Lambda_j$  with respect to a field direction  $\Phi$  in equation (4) is in general  $(ds_j/d\Phi) = -s_j \cdot \cos(\Omega + \Lambda_j - \Phi)$ . For structures oriented in the field direction  $\Omega = \Phi$  the sensitivity consequently simplifies as  $(ds_j/d\Phi) = -s_j \cdot \cos \Lambda_j$  for all exposable areas, and the term for lateral exposure sensitivity for a whole structure is the sum of elementary sensitivities:

$$\frac{dS_L(\Phi)}{d\Phi} = \sum_{\text{For all exposable areas}} -c_j \cdot s_j \cdot \cos(\Lambda_j) \quad (7)$$

The exposability of different properties and sensitivities for individual objects and compositions of structures of optional shapes are attainable in general by analytical, numerical, or graphical methods accounting for effects of hidden objects of structures where necessary.

#### 4.1. Surface exposability of rectangular objects

The note next illustrates the distributions of surface exposability in field directions  $S_L(\Theta) = \Omega$  of rectangular objects  $s_1 \times s_2$  with four elementary areas  $s_1, s_2, s_3, s_4$  [equation (5)] for different aspect ratios  $s_1/s_2$  in polar diagram (Fig. 5a) and in

normal diagram (Fig. 5b). Note how the shapes of objects significantly influence the structural exposability as well as the sensitivity to exposure.

#### 4.2. Surface exposability of an object on six piles

The surface exposability of an object on six rectangular piles (Fig. 6) is presented for the whole range of object's angle  $\Omega$  in polar diagram (Fig. 7a) and in normal diagram (Fig. 7b) using equations (4) and (6).

The outer (the upper) curves represent the fully exposed structure without hidden areas with overall aspect ratio 4/7. The inner (the lower) curves represent the lateral exposure when all interior areas are hidden behind the frontal objects with aspect ratio 2/3. The curves in between represent the lateral exposure if the background areas are hidden behind the frontal structures. The shadowed arrows illustrate the field effect at exposure of hidden object's parts (Fig. 6).

### 5. Effects of directional loading fields on marine objects and structures

The definition of directional exposability enables the assessments of the local and global effects of seasonally nonuniform loading fields on marine objects and structures. Thus, the directional exposure of an object  $E_s(\Phi, H_e, \Omega)$  during the season  $s$  in direction  $\Omega$  (Fig. 4) to the effect of a loading field in direction  $\Phi$  is in general modeled as the product of the field intensity  $F_s(\Phi, H_e)$  (e.g., Figs. 3a and 3b) and the object's exposability  $S(\Theta)$  [equations (5) or (6) and e.g., Figs. 7a and 7b]:

$$E(\Phi, H_e, \Omega) = F(\Phi, H_e) \cdot S(\Theta) \quad (8)$$

The design requirements or the operational observations may impose some characteristic field intensity values that significantly affect the structural exposure such as it could be, for example, the effective wave that exceeds the design height  $H_e$  in equation (8).

The study investigates in the sequel the meaning of the overall seasonal exposure of a structure in arbitrary position  $\Omega$  to that is definable by the integral of all the directional exposures  $E(H_e, \Omega)$  [equation (8)] in the whole range  $0 \leq \Phi \leq 2\pi$  for the specified effective wave height  $H_e$  during the season's period:

$$E(H_e, \Omega) = \int_{\text{All } \Phi} E(\Phi, H_e, \Omega) d\Phi \approx \sum_{\text{All } i} E(\Phi_i, H_e, \Omega) \quad (9)$$

It can be practical for numerical calculations to apply discrete field directions  $\Phi_i$  to define the overall seasonal exposure of a structure to field effect  $F(\Phi_i, H_e)$  in equation (9) instead of continuous as in equation (9).

The distribution of directional exposures  $e_i$  of marine objects and structures for all  $i$  [equation (8)] normalized to unity

$$\sum e_i(\Phi_i, H_e, \Omega) = 1$$

by employment of the overall seasonal exposure [equation (9)] can be obtained:

$$e_i(\Phi_i, H_e, \Omega) = E(\Phi_i, H_e, \Omega) / E(H_e, \Omega) \quad (10)$$

The entropy of the distribution of directional exposures  $e_i$  of marine objects and structures in equation (10), similarly as it is defined for the uncertainty of the distribution of wave directions in

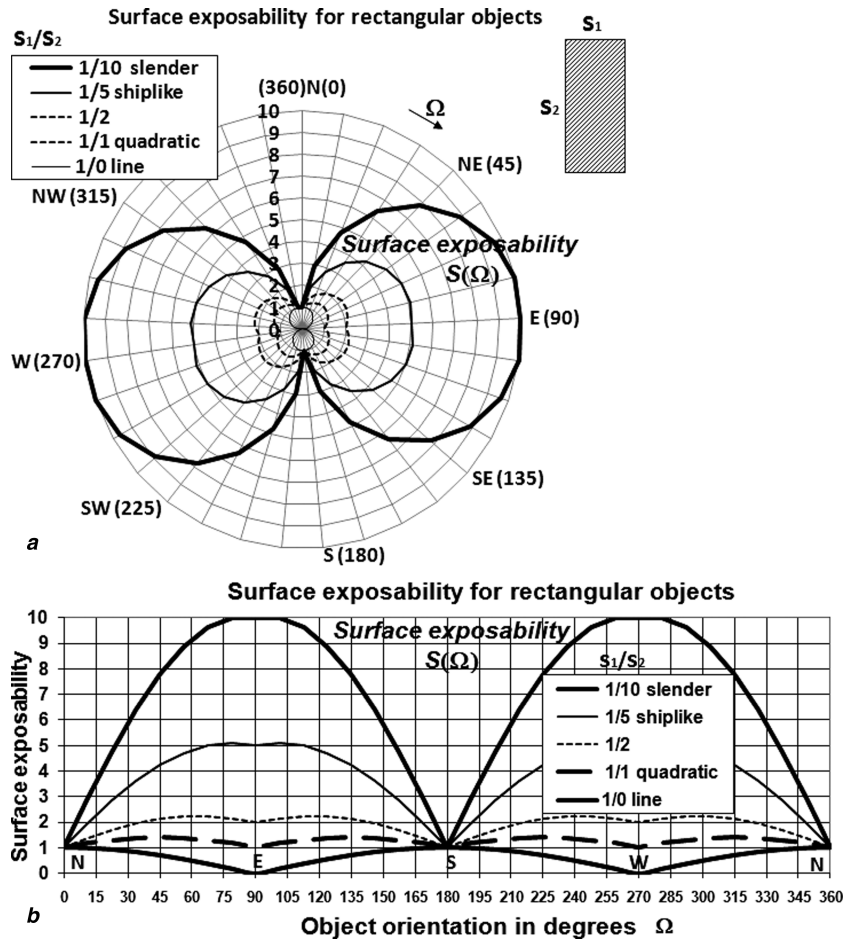


Fig. 5 a Polar presentation of surface exposability of rectangular structures for different aspect ratios. b Surface exposability of rectangular structures for different aspect ratios

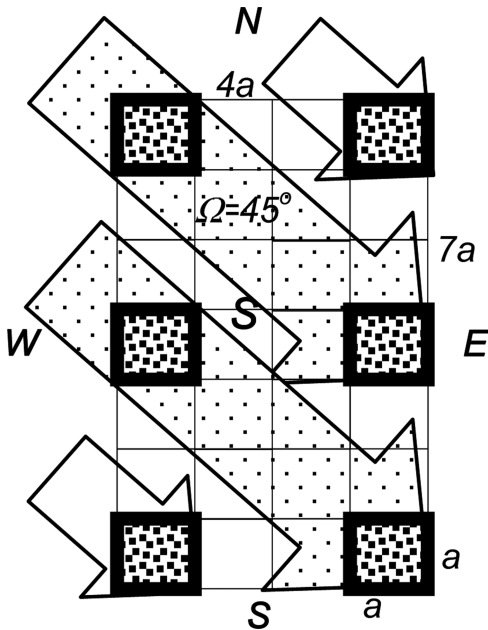


Fig. 6 Exposability of a marine object on six piles

equation (2), expresses the uncertainty, that is, the nonuniformity of the loading field effects. Since the uniform exposures to variable loading fields indicate robust behavior of marine objects, the following term may be viewed as a measure of robustness:

$$R(H, \Omega) = -\sum_{\text{all } i} e_i \log e_i \quad (11)$$

Robust positioning of marine objects with respect to the loading field is characterized with high value of entropy [equation (11)] that provides least nonuniformities of distribution of responses in the period of exposure to field effects.

## 6. Optimal position of stationary marine structures in loading fields

The worst case engineering reasoning normally imposes that the favorable short-term position of a structure  $\Omega_{\text{fav}}$  at a time is in the unfavorable direction of the loading field effect  $\Phi_{\text{unfav}}$  deducible from the directional exposure of marine objects and structures [equation (8)] in:

$$E(\Phi_{\text{unfav}}, H_c, \Omega_{\text{fav}}) = F(\Phi_{\text{unfav}}, H_c) \cdot S(\Phi_{\text{unfav}}, \Omega_{\text{fav}}) \quad (12)$$

The study also investigates the task of optimal long-term positioning of marine structures by using the concept of overall

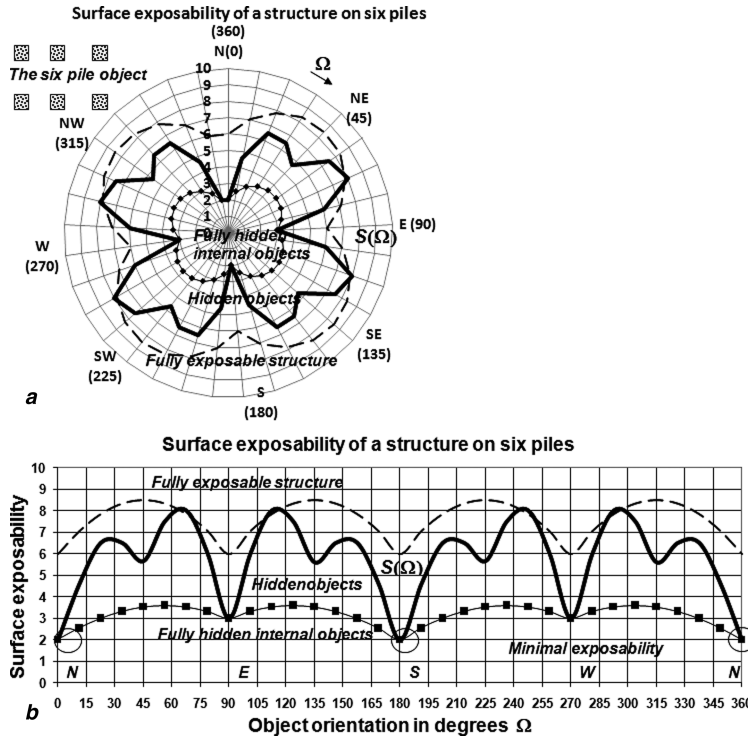


Fig. 7 a Polar diagram of surface exposability of an object on six piles (Fig. 6). b Normal diagram of surface exposure of an object on six piles (Fig. 6)

seasonal exposure to field effect [equation (9)] during the season's period in the form of an optimization task:

$$\text{Find } \Omega_{\text{fav}} \text{ that optimizes } E(H_e, \Omega) \text{ [equation(9)]} \quad (13)$$

satisfying all design and operational requirements

The optimization in equation (13) can be either minimization or maximization depending on the design or operational objectives that follows from functions and service conditions of marine objects and structure.

The study reveals next a novel criterion for robust, that is, most uniform distribution of seasonal exposure to loading field effects that corresponds to maximization of the entropy [equation (11)] of the distribution of directional exposures  $e_i$  of marine objects and structures in equations (10) and (11) in the form of following optimization task:

$$\text{Find } \Omega_{\text{fav}} \text{ that maximizes } R(H, \Omega) \text{ [equation(11)]} \quad (14)$$

satisfying all design and operational requirements

### 6.1. Placement of a marine object on six piles near the western Brazilian coast

The next example illustrates the selection procedure for the optimal positioning of the object on six piles (Fig. 6) based on its surface exposability (6) (Figs. 7a and 7b) in GWS area A67 in Atlantic Ocean near the east Brazilian coast (Appendix). The prevailing annual wave direction for all wave heights in area A67 is (SE) or  $\Phi_{\text{max}}=135$  deg, and the mean value in the field is  $\Phi_{\text{mean}}=120$  deg (Figs. 3a and 3b).

The worst case engineering approach [equation (12)] suggests that the favorable position of the object is its least directional

exposure to the most unfavorable direction of the loading field on annual basis, that is  $\Omega_{\text{fav}} = \Phi_{\text{unfav}} = 135$  deg.

The alternative procedure for long-term positioning of marine objects by minimization of the overall annual surface exposure to field effect [equation (13)] indicates the optimal direction of the object in the field as  $\Omega_{\text{fav}} = 125$  deg, that is between  $\Phi_{\text{max}}$  and  $\Phi_{\text{mean}}$  (Figs. 8a and 8b).

The novel procedure proposed by equations (11) and (14) for long-term robust positioning based on the entropy criterion of most uniform exposure or least uncertain service [equation (14)] indicates the optimal direction of the object in the field as  $\Omega_{\text{fav}} = 145$  deg (Figs. 8a and 8b).

The study supports the selections of criteria for assessments of directionally nonuniform wind and wave loading field effects on efficient placement of marine structures during the operation period that provide either a minimal overall exposure [equation (13)] or robust uniform distribution of exposures [equation (14)].

### 6.2. Lateral exposure of ship hull scantlings to wind wave loads

The next example considers a tanker with typical length  $L$  to breadth  $B$  ratio  $L/B = 5.6$  that is for example convertible into FPSO. The study investigates the directional exposure of the shell plating and supporting structures to lateral static and dynamic wave effects and accordingly the local strength of the ship's hull exposed to nonuniform wave impact loads.

The rule-based long-term dynamic envelope pressures  $P_{\text{ex-dyn}}$  for scantling requirements and strength assessment are given at a  $10^{-8}$  probability level, taking into consideration the effect of all wave headings (IACS 2008). The longitudinal factor  $f_{\text{lng}}$  defines the lengthwise distribution of design dynamic wave envelope



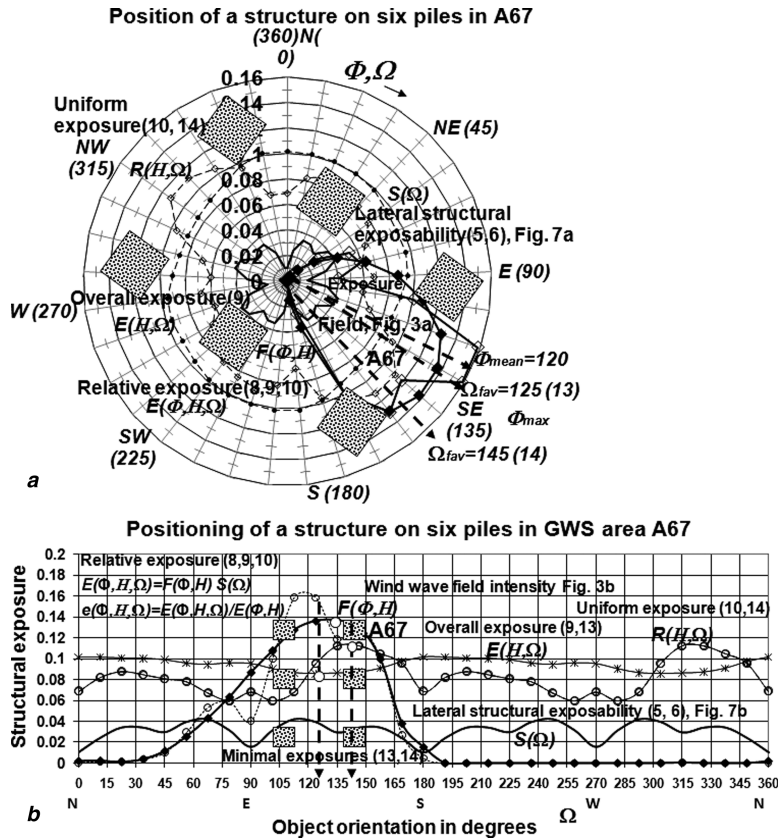


**Fig. 8** a Direction of minimal overall surface exposure of the object on six piles (Fig. 5) in the loading field in Marsden's square A67 (Fig. 2a) polar presentation. b Direction of minimal overall surface exposure of the object on six piles (Fig. 5) in the loading field in Marsden's square A67, normal presentation

pressures  $P_{ex-dyn}$  on hull that is increasing toward the ship's ends because of the wave impact loads (Fig. 9). Intermediate values to be obtained by interpolation.

The design scantlings need to be locally strengthened in proportion to the lengthwise distribution of design wave envelope pressures (factor  $f_{ing}$ ) (Fig. 9). The overall lateral directional exposability factor  $c$  [equation (5)] of the ship hull to wave loads at a time is therefore reduced in proportion to the lengthwise

distribution of the local strengthening  $c = 1/f_{ing}$ , particularly at the ship's ends (e.g., Fig. 9). The ship's length  $L$  in the range  $90 < L < 300$  affects the external long-term dynamic wave loads by wave coefficient  $C_{wv}$  (Fig. 10):

$$C_{wv} = 10.75 - \left( \frac{300 - L}{100} \right)^{3/2} \quad (15)$$

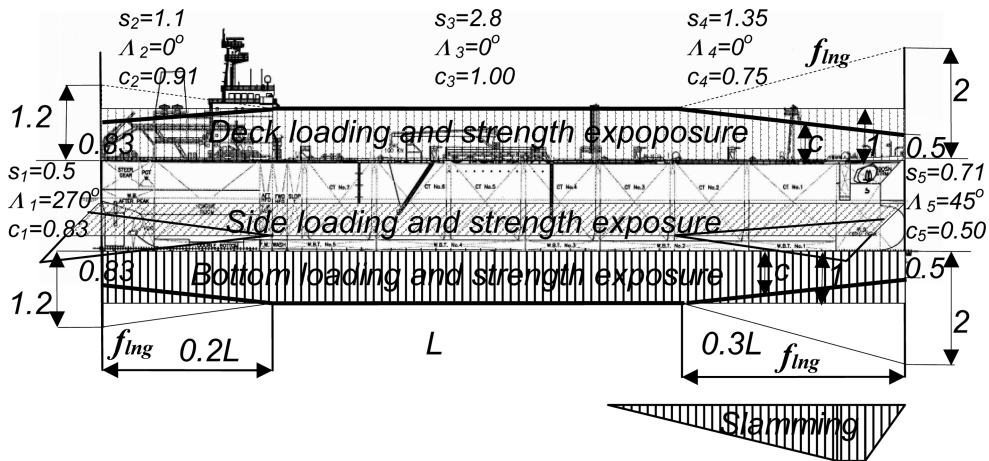


**Fig. 9** Rule-based long-term longitudinal distribution of lateral wave pressures and local scantlings exposability of a tanker to wave impact loads

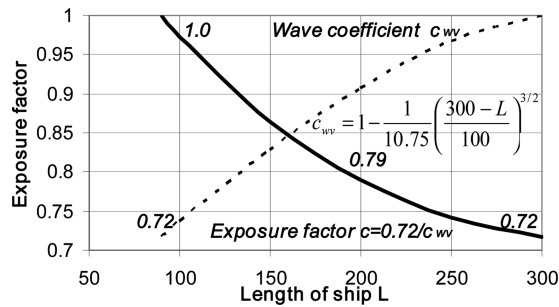


Fig. 10 Effect of ship size (length  $L$ ) on hull scantlings exposure to waves [equation (15)]

Results of overall lateral exposure calculations (5) for length to breadth ratio ( $L/B$ ) = 5.6 are standardized between minimal and maximal exposures using the long-term wave pressure distribution along the ship's hull (Fig. 9) and the wave coefficient [equation (15)] (Fig. 10) for ships of  $L = 90, 200,$  and  $300$  m (Fig. 11). The ship's sides are most exposed since they are not equipped for direct wave impact loads. The ship's bow is least exposed because it is particularly strengthened to be fit for service for all load cases also including strengthening of bottom forward for slamming in ballast conditions (Fig. 11). Bigger ships (90, 200, 300) are built stronger; that is, they are less exposed at a time to same wave fields in counter proportion to the wave coefficient  $C_{wv}$  [equation (15)] as 1.0/0.79/0.72 (Figs. 10 and 11). Note also that the  $L/B$  can significantly affect the ship's sensitivity to exposure [equation (5)] (Figs. 5a and 5b).

The sensitivity of the lateral exposure is highest at bow when the hull exposure is minimal (Fig. 11) implying that even small deviation of the direct heading into waves significantly increases the exposure. For example, the fluctuation of  $\Delta\Omega = \pm 45$  deg ( $1/4$ ) of the ship directions from the optimal heading into waves increases the hull exposure for 70%, 55%, and 50% for ship length  $L = 90, 200,$  and  $300$  m, respectively. Or, the increase of the ship exposure up to 50% occurs within  $\Delta\Omega = \pm 30, 40,$  and  $45$  deg of fluctuations in ship direction for appropriate ship length (Fig. 11).

The amount of exposure of scantlings to waves can be used as operational recommendations for the required directional control. The sustainable ship deviations of the optimal heading can be related to the tolerable hull exposure (Fig. 11) and wave heights with respect to the design wave height (Fig. 12). For example, for ships of  $L = 200$  m in length, the sustainable heading deviation

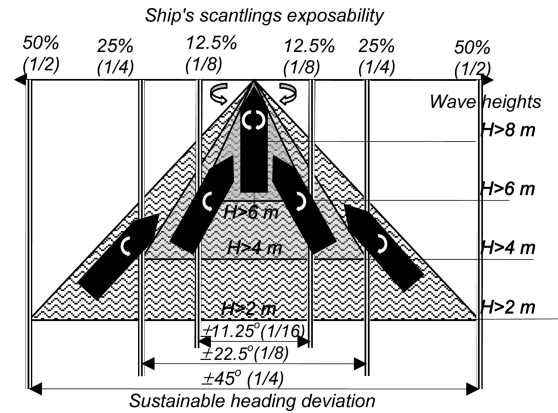


Fig. 12 Sustainable directional control with respect to ship's hull exposure

in waves above 2 m in height is recommended to be within  $\Delta\Omega = \pm 45$  deg ( $< 1/4$ ) (Fig. 12), which implies that the relative exposure is not exceeding 55% ( $\sim < 1/2$ ) (Fig. 11). Scaled accordingly, in waves above 4 m deviation should not exceed  $\Delta\Omega = \pm 22.5$  deg ( $1/8$ ) for 25% ( $1/4$ ) exposure and in waves above 6 m should not exceed  $\Delta\Omega = \pm 11.25$  deg ( $1/16$ ) for 12.25% ( $1/8$ ) exposure (Fig. 11). The recommendations for exposure-based directional control may be adjusted with respect to the observations in the field and practical experience during the operational period.

The ship is next exposed for example to the nonuniform wind wave loading field in the Gulf of Mexico. This field is appropriate to the Marsden's square A32 in GWS where the annual average number of wave directions is 6.4 out of 8 possible (Fig. 2, Appendix). The wave loading field in area A32 on annual basis characterizes a bimodal distribution of wave heights against directions (Fig. 13) that clearly differentiates the winter and summer seasons. Waves above 9 m are observed only in directions NW (31%) to N (69%) during the winter season December–February (DF). Waves above 6 m are observed in directions NW to NE (about 90%). The waves about 4 m and below prevail in the summer season June–August (JA) in directions NE to SE (about 80%).

The quantification of the ship exposure from 0% to 100% (Fig. 11) can provide a guideline that brings together the limiting wave heights for directional control and the seasonal climatologic observations. The usage of exposure information may help to predict the ship seasonal service conditions in operation fields.

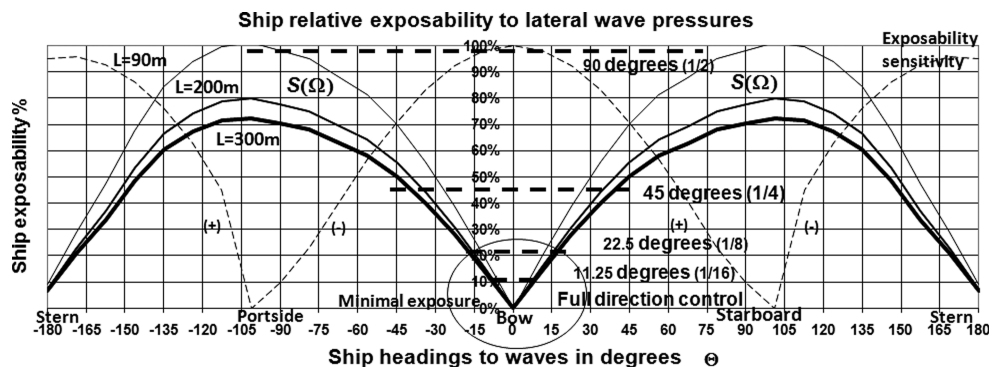


Fig. 11 Relative exposure of ship hull scantlings and the sensitivity to lateral wave loads

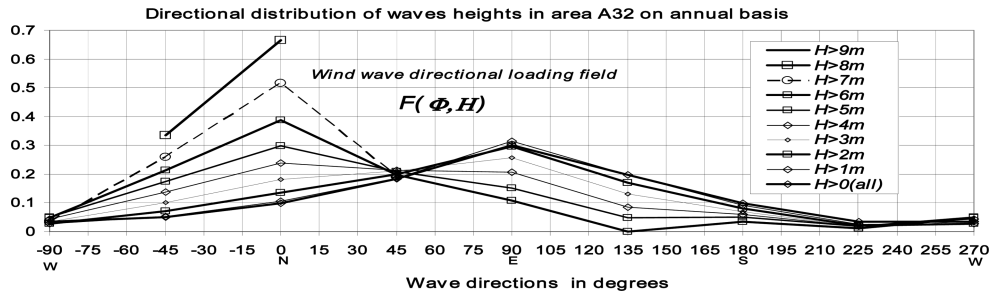


Fig. 13 Distribution of wave directions for wave heights in the Gulf of Mexico on annual bases

For example, during the summer season (JA) in the Gulf of Mexico of all the waves 87% are below 2 meters (Fig. 13). This is an indication that smaller ships about 90 m have to control their directions within  $\pm 45$  deg ( $1/4$ ) since most of the time the bigger ships over 200 m do not need additional direction control. Moreover, the ships in summer time will be positioned in prevailing direction E since about 90% of waves below 2 m are in directions from NE to SE (Fig. 13).

In the winter season (DF) about 12% of waves exceed 4 m mostly in directions from NW to NE (85%). Smaller ships below 200 m that are more exposed to wave impact loads will hardly cope with the required direction control in severe winter weather conditions. The ships more than 200 m in length might have about 20 deg ( $\Delta\Omega = \pm 20, \sim 1/8$ ) freedom for direction control. Most of the time (about 85%) during the harsh winter ships are highly exposed to waves exceeding 5 m in height and should be positioned in the directions between NW and NE (Fig. 13). Other sources for wave climate than GWS can also be used (Young & Holland 1996, Metocean).

### 6.3. Directional exposures of a ship hull

The study next considers some qualitative aspects of the wind wave loading field directional effects and their combinations on the local and global level, such as, for example, are the joint directional influences of lateral dynamic loads, ship's motions as a rigid body, and the ship's strength or deflections as a hull girder (Fig. 14).

The variety of field effects and responses as well as their combinations on one hand require appropriate decision about optimal or at least sustainable placement or headings to waves. On the other hand, the avoidances of unfavorable field effects are at least as important as the selection of the favorable service conditions.

Single-criterion approach for evaluation of ship service in nonuniform conditions may be appropriate when there is a recognized dominant exposure  $E(\Phi, H, \Omega)$  [equation (8)] expressible by explicit requirements on object's favorable exposable  $S_n(\Theta)$  [equation (5)] for given circumstances in a wind wave field  $F(\Phi, H)$ , for example:

- Minimize local wind wave impact loads or responses (stresses, deflections, fatigue, vibrations)
- Minimize global forces or responses (normal and shear stresses, hull deflections in sagging and hogging conditions, ultimate strength, fatigue)
- Minimize motions (e.g., rolling, pitching, heaving) or responses (stability degradation, accelerations, loss of speed in waves).

Complex ship service that includes different combinations quantifiable through  $N$  exposures  $E_n(\Phi, H, \Omega)$ ,  $n = 1, 2, \dots, N$  in [equation (8)] to a number of field effects may be tackled by multicriteria, multiobjective, or multiattribute methods from operations research with a number of constraints on structural exposable  $S_n(\Theta)$  [equations (5) or (6)] to resolve the conflicting service and other operational conditions.

Different decision-making techniques (e.g., Bernard 1996, Collette & Siarry 2004, Yoon & Ching-Lai 2006) are to be applied for more than one significant field effect  $n = 1, 2, \dots, N$  such as local, global, transverse, longitudinal, internal, external, strength, motions, accelerations, stability, slamming, sloshing, bow impact, loss of speed as well as general safety and reliability of different load cases in all conditions.

The study next illustrates the multicriteria approach to combined field effects by weighted sum of standardized exposable criteria where the weights  $w_n$  represent the influencing factors

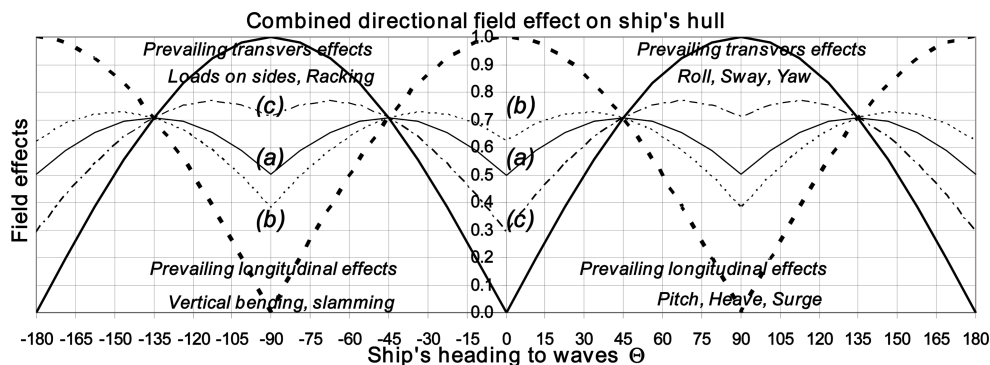


Fig. 14. Relative local and global directional effects of nonuniform loading fields on ships

either of objective nature if available or assessed by subjective or empirical judgment when not exactly known. The influencing factors  $w_n$  for combination of  $N$  exposures represent the relative importance of relevant criteria for predefined quality of operations and safe service concerning with exposability  $S_n(\Theta)$  to variable field effects (Table 2):

$$C(H, \Phi) = \sum_{n=1}^N w_n \cdot S_n(\Theta) \quad (16)$$

The study considers two groups of predominantly external local and global wind wave field effects: the prevailing transverse effects (impact loads on sides, racking, roll, sway, and yaw) and the predominantly longitudinal effects (hull bending, slamming, pitch, heave, and surge), altogether  $N = 10$  in equation (16) (Table 2).

The ship's exposure to wind and waves affects service conditions, navigation, sustainable speed, mooring, maneuvering, cargo handling, as well as offshore and onshore activities. The waves influence lateral, in-plane, or cross-sectional properties either of superstructures or of underwater bodies of ships. The waves also affect the local and global ship responses (loads, deformations, motions, and accelerations), longitudinal, transverse, and general directional features, structural integrity, safety, reliability, vulnerability, seakeeping, stability, fatigue, comfort, as well as the short-term and overall long-term fitness for service. The exposure of the ship to waves depends on types, size, and operational profile of ships and has consequences for the ship's lifetime, owner and crew satisfaction, operational hazards, service efficiency, and maintainability.

The combination of all field effects with supposedly equal influences on ship service (Table 2, column *a*) indicates that the favorable minimal ship's hull exposure is equal both for the ship heading into waves and in transverse direction to the waves (Fig. 14, curve *a*). Put succinctly the direction selection in waves is irrelevant for ship service.

The prevailing importance of transverse effects has influence on reduction of exposabilities to impact loads on sides, racking, roll, sway, and yaw (Table 2, column *b*). Accordingly, the favorable minimal ship's hull exposure is in ship's transverse direction to the waves (Fig. 14, curve *b*).

The prevailing importance of longitudinal effects requires low exposabilities to hull bending, slamming, pitch, heave, and surge (Table 2, column *c*). Consequently, the favorable minimal ship's hull exposure is for the ship heading into waves (Fig. 14, curve *c*).

**Table 2 Subjective weighting factors  $w_n$  for combinations of loading field effects (16)**

Effect	(a)	(b)	(c)
Impact on sides	1	1	2
Racking	1	0.2	0.4
Roll	1	2	4
Sway	1	0.1	0.2
Yaw	1	0.1	0.2
Bending	1	2	1
Slamming	1	1.6	0.8
Pitch	1	1	0.5
Heave	1	0.8	0.4
Surge	1	0.2	0.1
Direction	Irrelevant		Heading

For all the combination of operational conditions at sea it is possible to identify the unfavorable directions where the combined effects are maximal (Fig. 14).

## 7. Conclusion

Important aims of engineering efforts in design, service, and maintenance of marine objects are to maximize the lifetime fitness for service accounting for structural exposability to seasonal loading field variability. In practice decisions due to changes of service conditions are often left to intuition and experience. However, complex maritime service may entail a more sophisticated approach with a number of design, structural, and operational constraints on structural exposability to resolve conflicting service and other operational requirements in variable operational conditions by compromising solutions.

The methods based on variability of distributions of probabilities and on probabilistic entropy of systems of observations of wind wave directions facilitate the identification and presentation of loading field nonuniformities that can affect design, service, and maintenance of marine objects and structures. Significant loading field variations are recognizable from attached global chart of ocean wind wave directional nonuniformities of all GWS ocean areas. Evidently the global wind wave climate induces significant differences in loading fields that seasonally influence marine objects depending on the service area.

The loading field identification procedures are applicable to other sources of local and global wave properties as well as for available empirical or theoretical probability distributions of wave heights, periods, and direction. Such sources for example are the *Atlas of the Oceans: Wind and Wave Climate* prepared by Young and Holland (1996) and recently the remotely accessible more objective satellite measurements in the Metocean climate atlas (CLIOSat), Integrated Marine Decision Support System (IMDSS), Global Ocean Observing System (GOOS) under auspices of World Meteorological Organization (WMO) and in Intergovernmental Oceanography Commission (IOC).

The directional exposability of superstructures and underwater bodies of stationary as well as of nonstationary marine objects can be calculated as their external or internal property for responding to local or global effects of directionally nonuniform loading fields during seasonal service. Directional expositions of individual marine structures as well as the marine structures of several similar or different objects that can mutually interact are presented in polar and normal diagrams.

The directional distributions of wind wave loading fields and the directional distributions of structural exposability jointly define the exposures of marine objects that inspire the attempt toward optimal placement and selection of sustainable directions of marine structures in directionally variable loading fields.

The study applies two criteria for favorable positioning of marine structures: the criterion of optimal overall seasonal exposure and the criterion of robust, that is, most uniform distribution of seasonal exposure to the whole range of wave loading field directions of interests in the lifetime. The application of criteria of minimal or most uniform exposure ensures that the marine structures during lifetime or seasonal service expose the most resistant parts of the structure to the worst field effects and the most vulnerable parts of a structure to the least field effects.

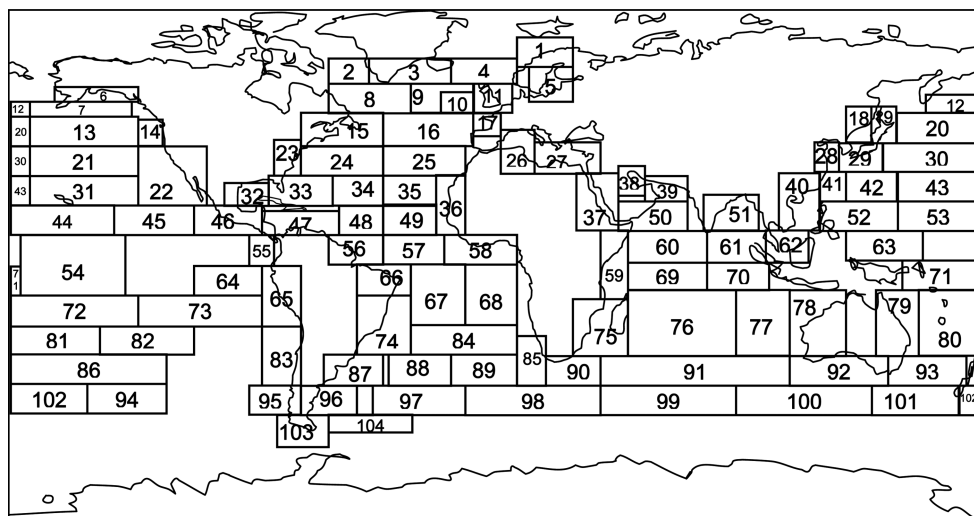
The two criteria provide a background for a methodology for numerically fast and empirically reasonable explicit or compromising solutions for placement of marine structures in directionally nonuniform wave loading fields.

Combinations of various wind wave loading field influences on the local and global level in transverse and longitudinal direction, such as, for example, the joint directional influence of lateral static and dynamic loads, ship's motions as a rigid body and the ship's strength as a hull girder are important for successful missions at seas. The variety of field effects on one hand requires multiple criteria decisions about optimal or at least sustainable placement or headings to waves of objects and structures. On the other hand, suggestions for avoidance of unfavorable field effects are at least as important as the selection of favorable service conditions. Compromising might be often necessary.

The definition of directional distributions of complex properties of marine structures, such as the local/global strength and stability/motions/accelerations normally requires difficult computational procedures. Instead, the study investigates simplified methodologies for optimal placement of marine structures by applying their directional exposability in combination with variability of uncertain loading fields. The study generally puts emphasis on simplicity in defining the exposability of marine objects and on convenience of practical numerical procedures for exposure forecast, optimal placement, and selection of sustainable directions in directionally and seasonally variable loading fields.

## References

- ACZEL, J., AND DAROCZY, Z. 1975 *On Measures of Information and Their Characterization*, Academic Press, NY.
- BERNARD, R. 1996 *Multicriterial Methodology for Decision Aiding*, Springer-Verlag, New York.
- BELENKIY, L., AND RASKIN, Y. 2001 Estimate of the ultimate load on structural members subjected to lateral loads, *Marine Technology (SNAME)*, **38**, 3, 169–176.
- COLLETTE, Y., AND SIARRY, P. 2004 *Multiobjective Optimization: Principles and Case Studies*, Springer-Verlag, New York.
- EWING, J.A. 1990 Wind, wave and current data for the design of ships and offshore structures, *Marine Structures*, **3**, 6, 421–459.
- GERWICK, B. C., AND MORRIS, M. D. 2007 *Construction of Marine and Offshore Structures*, CRC Press, Boca Raton, FL.
- GUEDES SOARES, C. 2003 Wave-induced loads in marine structures, *Marine Structures*, **16**, 2, 95–99.
- GUMDESTAD, O. T. 1993 Measured and predicted deep water wave kinematics in regular and irregular seas, *Marine Structures*, **6**, 1, 1–73.
- HOGBEN, N., DACUNHA, N. M. C., AND OLLIVER, G. F. 1986) *Global Wave Statistics*, British Maritime Technology Ltd., Feltham.
- IACS 2008 *Common Structural Rules for Double Hull Oil Tankers*, IACS, Germanischer Lloyd AG, Hamburg, Germany.
- KHINCHIN, A. I. 1957 *Mathematical Foundations of Information Theory*, Dover Publications, New York.
- MAVRAKOS, S. A., PAPAZOGLU, V. J., TRIANTAFYLLOU, M. S., AND HATIGEORGIOU, J. 1996 Deep water mooring dynamics, *Marine Structures*, **9**, 2, 181–209.
- Metocean data collection, <http://www.metocean.com/>.
- NOBLESSE, F., YANG, C. 1993 An approach to the calculation of wave loads on ships and floating structures, *Marine Structures*, **6**, 2–3, 223–239.
- PAIK, J. K. 2006 Toward limit state design of ships and offshore structures under impact pressure actions: A state-of-the-art review, *Marine Technology (SNAME)*, **43**, 3, 135–145.
- PAIK, J. K., AND THAYAMBALLI, A. K. 2007 *Ship-Shaped Offshore Installations (Design, Building, and Operation)*, Cambridge University Press, Cambridge, U.K.
- RENYI, A. 1970 *Probability Theory*, North-Holland, Amsterdam, The Netherlands.
- SHANNON, C. E., AND WEAVER, W. 1949 *The Mathematical Theory of Communication*, Urbana University, Urbana, IL.
- SII, H. S., WANG, J., ELEYE-DATUBO, A. G., YANG, J. B., AND LIU, J. 2005 Safety assessment of FPSO turret-mooring system using approximate reasoning and evidential reasoning, *Marine Technology (SNAME)*, **42**, 2, 88–102.
- WILSON, J. F. 2002 *Dynamics of Offshore Structures*, 2nd ed., Wiley.
- WIENER, N. 1948 Cybernetic, or control and communication, *The Bell System Technical Journal*, **27**.
- YOUNG, I. R., AND HOLLAND, G. J. 1996 *Atlas of the Oceans: Wind and Wave Climate*, Pergamon.
- YOON, K. P., AND CHING-LAI H. 2006 *Multiple Attribute Decision Making: An Introduction*, Sage Publications, Thousand Oaks, CA.
- ZIHA, K. 2000a Event oriented system analysis, *Probabilistic Eng. Mech.*, **15**, 3, 261–275.
- ZIHA, K. 2000b Redundancy and robustness of systems of events, *Probabilistic Eng. Mech.*, **15**, 4, 347–357.
- ZIHA, K. 2007 Entropy of marginal distributions. In: Luzar-Stiefler V, Hljuz Dobrić V, editors. *Proceedings 29th International Conference on Information Technology Interfaces*, IEEE Catalog No. 07EX1589C; Cavtat, Croatia. Zagreb: SRCE University Computing Centre, University of Zagreb.



Appendix: Marsden squares in GWS by Hogben et al (1986)